Single-cell transcriptome analysis of human skin identifies novel fibroblast subpopulation and enrichment of immune subsets in atopic dermatitis

Helen He, BS,[a]* Hemant Suryawanshi, PhD,[b]* Pavel Morozov, PhD,[b] Jesús Gay-Mimbrera, PhD,[c] Ester Del Duca, MD,[a] Hyun Je Kim, MD, PhD,[a] Naoya Kameyama, PhD,[a] Yeriel Estrada, BS,[a] Evan Der, BS,[d] James G. Krueger, MD, PhD,[e] Juan Ruano, MD, PhD,[c] Thomas Tuschl, PhD,[b] and Emma Guttman-Yassky, MD, PhD[a] *New York, NY, and Córdoba, Spain*

GRAPHICAL ABSTRACT

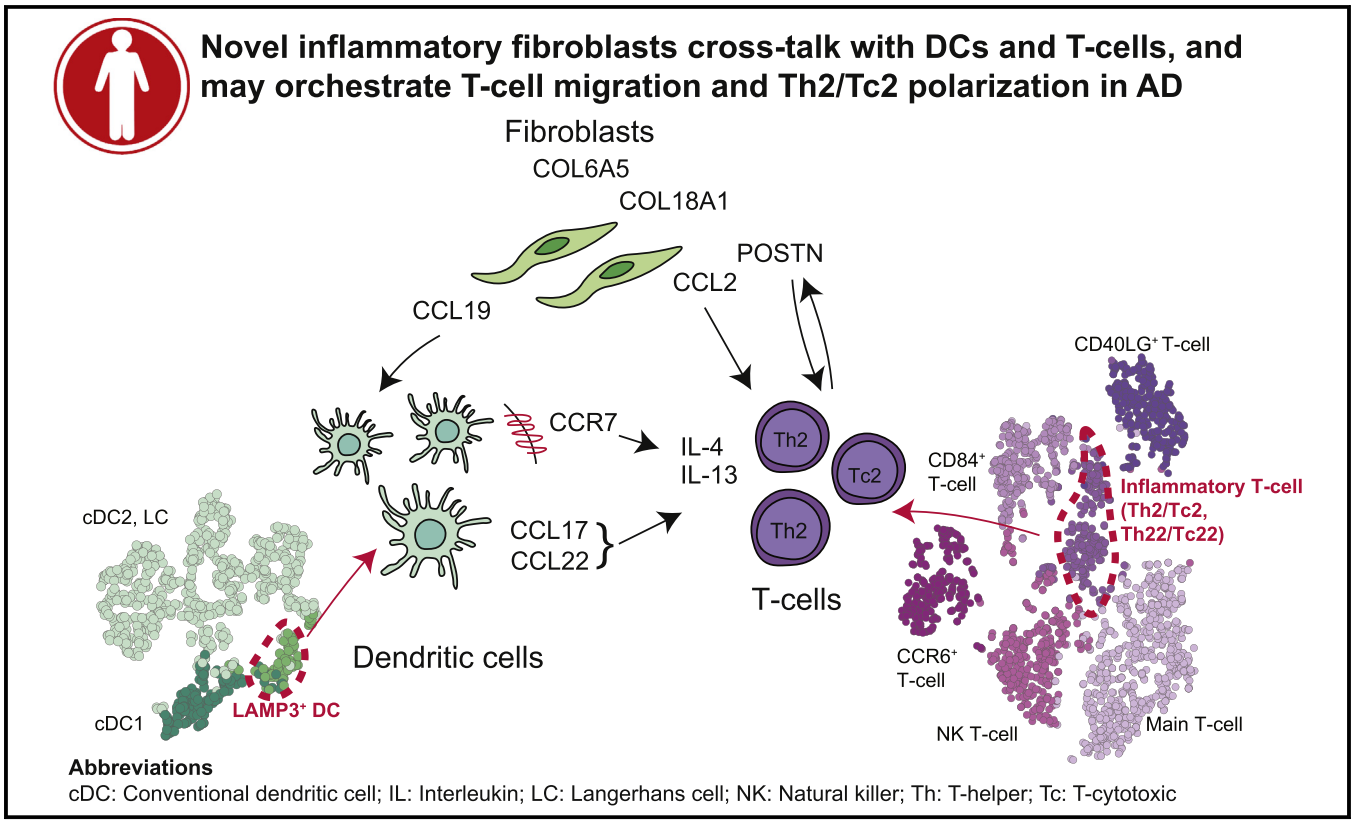

From [a]the Department of Dermatology, Icahn School of Medicine at Mount Sinai, New York; [b]the Laboratory of RNA Molecular Biology and [e]the Laboratory of Investigative Dermatology, The Rockefeller University, New York; [c]the Department of Dermatology, Reina Sofía University Hospital, Córdoba; and [d]the Division of Rheumatology and Department of Microbiology and Immunology, Albert Einstein College of Medicine, New York.

*These authors contributed equally to this work.

Disclosure of potential conflict of interest: J. G. Krueger is an employee of Rockefeller University and has received research support (grants paid to his institution) and/or personal fees from Pfizer, Amgen, Janssen, Lilly, Merck, Novartis, Kadmon, Dermira, Boehringer, Innovaderm, Kyowa, BMS, Serono, BiogenIdec, Delenex, AbbVie, Sanofi, Baxter, Paraxel, Xenoport, and Kineta. E. Guttman-Yassky is an employee of Mount Sinai and has received research funds (grants paid to her institution) from AbbVie, Celgene, Eli Lilly, Janssen, Medimmune/Astra Zeneca, Novartis, Pfizer, Regeneron, Vitae, Glenmark, Galderma, Asana, Innovaderm, Dermira, and UCB and is also a consultant for Sanofi Aventis, Regeneron, Stiefel/GlaxoSmithKline, MedImmune, Celgene, Anacor, AnaptysBio, Dermira, Galderma, Glenmark, Novartis, Pfizer, Vitae, Leo Pharma, AbbVie, Eli Lilly, Kyowa, Mitsubishi Tanabe, Asana Biosciences, and Promius. The rest of the authors declare that they have no relevant conflicts of interest.

Received for publication August 13, 2019; revised January 15, 2020; accepted for publication January 21, 2020.

Available online February 7, 2020.

Corresponding author: Emma Guttman-Yassky, MD, PhD, Department of Dermatology and Laboratory of Inflammatory Skin Diseases, Icahn School of Medicine at Mount Sinai Medical Center, 5 E 98th St, New York, NY 10029. E-mail: emma.guttman@mountsinai.org. Or: Hemant Suryawanshi, PhD, Laboratory of RNA Molecular Biology, The Rockefeller University, 1230 York Avenue, New York, NY, 10065. E-mail: hsuryawans@mail.rockefeller.edu. Or: Thomas Tuschl, PhD, Laboratory of RNA Molecular Biology, The Rockefeller University, 1230 York Avenue, New York, NY, 10065. E-mail: ttuschl@rockefeller.edu.

0091-6749/$36.00

https://doi.org/10.1016/j.jaci.2020.01.042

Background: Atopic dermatitis (AD) is a prevalent inflammatory skin disease with a complex pathogenesis involving immune cell and epidermal abnormalities. Despite whole tissue biopsy studies that have advanced the mechanistic understanding of AD, single cell–based molecular alterations are largely unknown.

Objective: Our aims were to construct a detailed, high-resolution atlas of cell populations and assess variability in cell composition and cell-specific gene expression in the skin of patients with AD versus in controls.

Methods: We performed single-cell RNA sequencing on skin biopsy specimens from 5 patients with AD (4 lesional samples and 5 nonlesional samples) and 7 healthy control subjects, using 10× Genomics.

Results: We created transcriptomic profiles for 39,042 AD (lesional and nonlesional) and healthy skin cells. Fibroblasts demonstrated a novel *COL6A5*$^+$*COL18A1*$^+$ subpopulation that was unique to lesional AD and expressed *CCL2* and *CCL19* cytokines. A corresponding *LAMP3*$^+$ dendritic cell (DC) population that expressed the *CCL19* receptor *CCR7* was also unique to AD lesions, illustrating a potential role for fibroblast signaling to immune cells. The lesional AD samples were characterized by expansion of inflammatory DCs (*CD1A*$^+$*FCER1A*$^+$) and tissue-resident memory T cells (*CD69*$^+$*CD103*$^+$). The frequencies of type 2 (*IL13*$^+$)/type 22 (*IL22*$^+$) T cells were higher than those of type 1 (*IFNG*$^+$) in lesional AD, whereas this ratio was slightly diminished in nonlesional AD and further diminished in controls.

Conclusion: AD lesions were characterized by expanded type 2/type 22 T cells and inflammatory DCs, and by a unique inflammatory fibroblast that may interact with immune cells to regulate lymphoid cell organization and type 2 inflammation. (J Allergy Clin Immunol 2020;145:1615-28.)

Key words: *Atopic dermatitis, single-cell RNA sequencing, fibroblasts, dendritic cells, T cells, cytokines*

Abbreviations used

AD: Atopic dermatitis
CCL: CC chemokine ligand
cDC: Conventional dendritic cell
cDC1: Type 1 conventional dendritic cell
cDC2: Type 2 conventional dendritic cell
CXCL: C-X-C motif ligand
DC: Dendritic cell
DEG: Differentially expressed gene
ECM: Extracellular matrix
FB1: Type 1 fibroblast
FB2: Type 2 fibroblast
FB3: Type 3 fibroblast
IRS: Inner root sheath
KC1: Type 1 keratinocyte
KC2: Type 2 keratinocyte
KC3: Type 3 keratinocyte
LC: Langerhans cell
LEC: Lymphatic endothelial cell
NC: Neuronal cell
POSTN: Periostin gene
SC: Schwann cell
scRNA-seq: Single-cell RNA sequencing
SGC: Sweat gland cell
TEWL: Transepidermal water loss
TPM: Transcripts per kilobase million
T_{RM}: Resident memory T cell
VEC: Vascular endothelial cell
vSMC: Vascular smooth muscle cell

Atopic dermatitis (AD) is a common inflammatory skin disease, affecting 7% of adults and 15% of children in the United States.[1,2] AD involves skin immune and barrier abnormalities, including T-cell and dendritic cell (DC) infiltration,[3,4] epidermal hyperplasia, and disrupted keratinocyte differentiation.[4,5] AD is primarily characterized by a type 2 immune response,[3] but it may also involve type 1, 17, and 22 pathways to varying degrees.[6-8] In patients with moderate-to-severe AD, defined as involving more 10% of the body surface area, these abnormalities extend beyond the visibly affected skin to also involve nonlesional skin.[9]

Until recently, skin profiling was based solely on characterization of bulk tissue skin biopsy specimens, with use of transcriptomic profiling approaches such as RNA sequencing and microarrays to provide insights into AD pathogenesis.[10,11] Although whole skin biopsy specimens provided important information on the cytokine profile, they did not readily define the originating cell types. Single-cell RNA sequencing (scRNA-seq) offers a novel approach to define the cellular composition in the skin, including novel or rare cell populations, that is able to resolve cell-specific changes in gene expression in patients with AD versus in controls. Current scRNA-seq studies in healthy skin are highly specific, focusing either on epidermal cells,[12] fibroblast subpopulations,[13,14] or the hair follicle.[15] Single-cell analysis of skin and kidney biopsy specimens from patients with lupus revealed important insights in resolving cell type–specific interferon-stimulated gene expression and fibrotic events that may have prognostic value.[16,17] To our knowledge, deep single-cell profiling by using the latest emulsion-capture technology with all epidermal and dermal cells in healthy skin is unavailable, and single-cell analysis of AD skin has never been reported.

Here, we report scRNA-seq analysis for 39,042 cells obtained from 3 conditions: lesional and nonlesional skin from patients with AD and skin from healthy individuals. We used established cell lineage markers to construct a comprehensive map of all cell types in healthy, nonlesional, and lesional AD skin. We evaluated both composition and gene expression of cells for each condition, including detailed characterization of specific immune cell subsets. Finally, we identified abundantly expressed receptors and ligands for each cell type to highlight putative intercellular communication in the skin microenvironment.

METHODS

Patient and sample information

Lesional and nonlesional skin biopsy specimens were taken from the extremities of 5 patients with moderate-to-severe AD (mean SCORing Atopic Dermatitis score, 68.7; mean Eczema Area and Severity Index, 20.7; mean Investigator's Global Assessment score, 3; mean body surface area, 44.4%; and mean eosinophil count, 500/μL) and 7 matching controls. All subjects provided institutional review board–approved consent. Patients with AD had chronic disease (age of onset <5 years), no topical steroid/immunomodulator use in the last week, no systemic immunosuppressants or phototherapy in the last 4 weeks, and no moisturizer use within 12 hours.

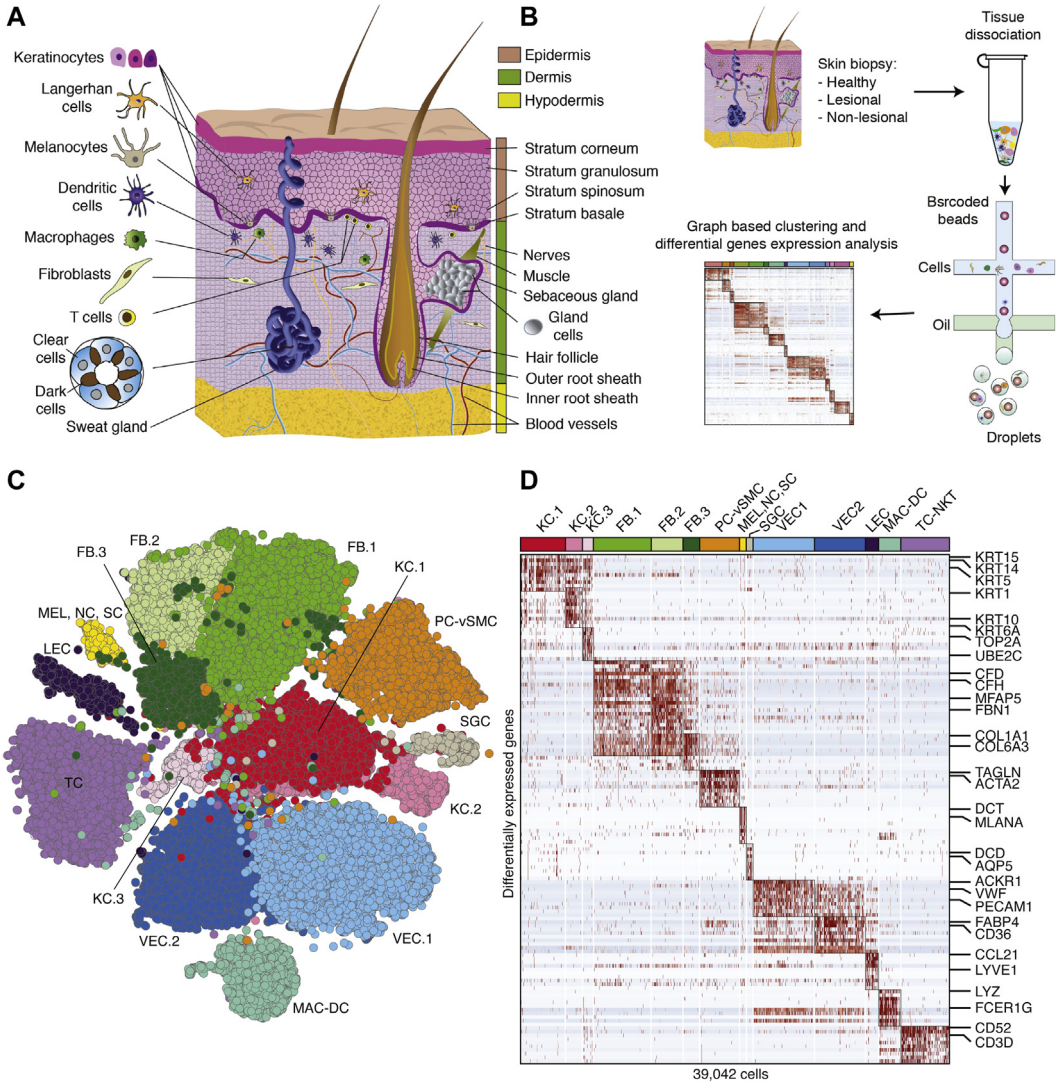

FIG 1. scRNA-seq atlas of cell populations in AD and healthy skin. **A,** Cross-sectional schematic illustrating diverse cell populations in skin. **B,** Workflow for single-cell profiling of skin, including biopsy specimen dissociation, droplet-based scRNA-seq, and graph-based clustering. **C,** t-Distributed stochastic neighbor embedding plot for 39,042 skin cells, derived from 5 patients with AD (4 lesional and 5 nonlesional samples) and 7 healthy subjects. **D,** Distinct gene signatures (top 10 differentially expressed genes; Wilcoxon rank sum test) of skin cell populations. *MAC,* Macrophage; *MEL,* melanocyte; *NC,* neuronal cell; *NKT,* natural killer T cell.

Single-cell capture, sequencing, and data processing

Biopsy specimens were cryopreserved, dissociated, and processed by 10× Genomics. The library was sequenced on the Illumina HiSeq 2500 platform to get approximately 150 to 200 million reads. The 10× raw data were processed by using the standard Drop-seq pipeline (http://mccarrolllab.com/dropseq/), with modifications.

Clustering analysis using Seurat and t-distributed stochastic neighbor embedding visualization

Clustering analysis using the Seurat package (version 2.3.4) was implemented for both first-level analysis across all cells and second-level higher-resolution analysis within cell types. ScRNA-seq data sets were combined into a single Seurat object and aligned by canonic correlation analysis to remove batch effects (see Fig E1, *A* in the Online Repository available at www.jacionline.org). Cells with fewer than 100 genes, more than 5000 genes, or more than 25% mitochondria content were excluded. Ubiquitously expressed ribosomal protein coding (ribosomal protein small and large units) and metastasis-associated lung adenocarcinoma transcript noncoding RNA, microRNA, and small nucleolar RNA genes were also excluded. The Wilcoxon rank sum test was used to identify differentially expressed genes (DEGs) in each cluster to define broad cell types and was then repeated for each resultant cell type to further characterize subpopulations. Read counts for each gene were normalized to 10,000 to generate transcripts per kilobase million (TPM)-like values. After canonic correlation analysis alignment, each cluster was represented by all samples (see Fig E1, *B-I*). Raw and processed scRNA-seq data for all samples have been deposited in the GEO database under accession code GSE147424 (https://www.ncbi.nlm.nih.gov/geo/query/acc.cgi?acc=GSE147424).

Composition, gene expression, and receptor-ligand interaction analyses

Pairwise comparisons were performed for all conditions by using an unpaired *t* test for lesional or nonlesional versus healthy samples, and a paired *t* test was used for lesional versus nonlesional samples. *SingleR* was used to

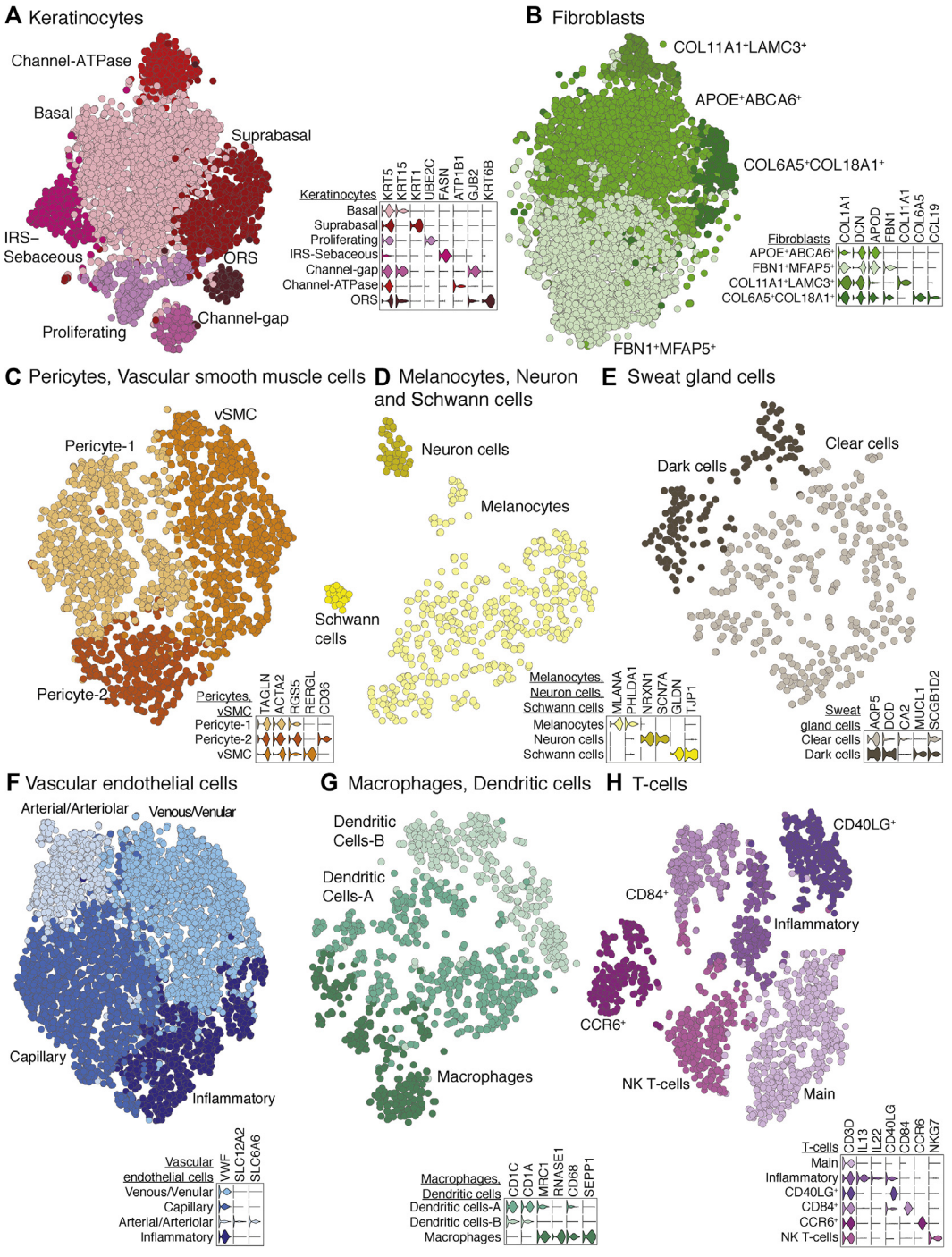

FIG 2. Heterogeneity of cell subpopulations in AD and healthy skin. t-Distributed stochastic neighbor embedding plots and accompanying violin plots of representative genes for keratinocytes (**A**); fibroblasts (**B**); pericytes and vascular smooth muscle cells (**C**); melanocytes, neuron cells, and Schwann cells (**D**); sweat gland cells (**E**); vascular endothelial cells (**F**); macrophages and DCs (**G**); and T cells (**H**). *NK*, Natural killer.

annotate T cells with fine-tuning by using the Human Primary Cell Atlas as the reference data set (http://biogps.org/dataset/BDS_00013/primary-cell-atlas/).[18] DEG analysis was performed by using *DESeq2*, with use of the criteria absolute value of log (fold change) greater than 1 and a false discovery rate less than 0.05. To identify potential intercellular interactions, we used a list of ligand-receptor pairs from the Database of Interacting Proteins (http://dip.doe-mbi.ucla.edu) and the International Union of Basic and Clinical Pharmacology/British Pharmacological Society guide to pharmacology (www.guidetopharmacology.org), as described earlier.[19] The list of interactions was intersected with the list of DEGs and with TPM-normalized gene levels (for details, see Table E1 and the Methods section in the Online Repository available at www.jacionline.org).

RESULTS

Strategy for scRNA-seq and data analysis

Cell suspensions, prepared on dissociation of cryostored skin biopsy specimens from 5 patients with AD (4 lesional and 5 nonlesional) and 7 controls, were subjected to droplet-based encapsulation (using × Genomics)[20] followed by library preparation and sequencing (Fig 1, *A* and *B*). Bioinformatics analysis identified 22,220, 10,169, and 6,653 high-quality scRNA-seq profiles from healthy, lesional AD, and nonlesional AD samples, respectively, which were aggregated and analyzed by graph-based clustering (Fig 1, *C* and *D*). Average expression profiles for each sample are listed in Table E1.

Cell type composition of healthy, nonlesional, and lesional skin

DEG analysis (Wilcoxon rank sum test) segregated 39,042 combined (healthy, lesional, and nonlesional) cells into 10 broad cell types: keratinocytes (KC1-KC3), fibroblasts (FB1-FB3), pericytes and vascular smooth muscle cells, melanocytes, NCs and Schwann cells (SCs), sweat gland cells (SGCs), vascular endothelial cells (VECs) (VEC1 and VEC2), lymphatic endothelial cells (LECs), macrophages and DCs, and T cells (Fig 1, *C* and *D* and see also Table E2 in the Online Repository available at www.jacionline.org). We determined the relative proportion of each cell type in all samples, showing increased immune cells in lesional AD versus in controls (see Fig E2 in the Online Repository available at www.jacionline.org).

Keratinocytes separated into 3 subpopulations by first-level t-distributed stochastic neighbor embedding analysis (Fig 1, *C* and *D*), but second-level analysis further separated them into 7 subpopulations, namely, basal, proliferating, suprabasal, inner root sheath (IRS)-sebaceous, outer root sheath, channel-ATPase, and channel-gap cells (Fig 2, *A*). Basal keratinocytes highly expressed *KRT5*, *KRT14,* and *KRT15*, whereas suprabasal keratinocytes specifically expressed early differentiation keratins (*KRT1 and KRT10*) and also highly expressed hyperproliferative (*KRT6A* and *KRT16*) and S100 (*S100A7* and *S100A8*) genes (see Fig E3, *A* in the Online Repository available at www.jacionline.org). Proliferating keratinocytes were characterized by expression of mitotic markers such as *UBE2C* and *TOP2A*. Sebaceous glands are lipid-producing epithelial cell structures that drain sebum to the infundibulum through a duct at the junction of infundibulum and isthmus.[21] A combined subpopulation of IRS and sebaceous gland cells (IRS-sebaceous) expressed *KRT79* and genes involved in lipid synthesis (*FASN*, *THRSP*, and *ELOVL5*), metabolism (*FADS2* and *ACSBG1*), and transport (*APOC1*). A cluster of $KRT6B^{+}KRT17^{+}$ keratinocytes corresponded to outer root sheath cells. Finally, 2 clusters expressed genes that regulate ion channels. "Channel-ATPase" expressed components of ATPases (*ATP1B1* and *ATP1A1*) and its regulators (*DEFB1* and *SAT1*), whereas "channel-gap" consisted of gap junctions, specifically expressing *GJB6*, *GJB2*, and *GJA1*.

Fibroblasts (FB1-FB3) expressed *COL1A1* and *DCN* and separated into 4 subgroups on second-level analysis (Fig 2, *B* and see Table E2). The 2 major FB populations both expressed lipid transport/homeostasis (*APOD*, *APOE*, and *ABCA6*) and complement genes (*C3*), but were distinguished by *FBN1* and *MFAP5* expression (Figs 2, *B* and E3, *B*). A third minor FB population expressed fibrocartilage- *(COL11A1)* and myofibroblast-related genes (*POSTN* and *EDNRA*), suggesting that they may be in a differentiating state. Finally, a previously unrecognized FB subtype expressed *COL6A5*, *COL6A6*, and *COL18A1*, along with chemokines *CCL2* and *CCL19*.

First-level analysis showed that pericytes and vSMCs expressed *TAGLN* and *ACTA2* (Fig 1, *C* and *D*), which further separated into type 1 and type 2 pericyte and vSMC clusters distinguished by expression of *RGS5*, *PDGFRB,* and *NOTCH3* and by *RERGL* and *CNN1*, respectively (Fig 2, *C* and see Fig E3, *C*). The population of type 2 pericytes had high expression of *CD36* and *FABP4*, suggesting their involvement in fatty acid transport across blood vessels.[22]

Melanocytes, neuronal cells (NCs), and SCs, which initially clustered together, formed separate clusters and were identified by the established lineage markers *MLANA*, *NRXN1*, and *GLDN*, respectively (Fig 2, *D* and see Fig E3, *D*). Interestingly, melanocytes expressed lipid transport (*APOE*) and cholesterol biosynthesis (*FDFT1*) genes, as well as the follicular stem cell marker *PHLDA1*. NCs expressed genes corresponding to sodium channels subunits (*SCN7A*), axons (*ANK3* and *SEMA3B*), and cell adhesion (*CADM1* and *CADM3*). SCs expressed the tight junction gene *TJP1*, Na^{+}/K^{+} ATPase regulator *FXYD6* and the creatine synthesis protein GATM.

SGCs that form the secretory coil are broadly of 2 secretory cell types: clear cells that secrete sodium chloride–rich sweat and dark cells that secrete glycoproteins and *DCD*/dermicidin).[23] Subclustering analysis differentiated clear from dark cells, respectively expressing *CA2* and *MUCL1* (Fig 2, *E* and see Fig E3, *E*). Although all SGCs expressed secretoglobins such as *SCGB1D2* and *SCGB2A2*, only dark cells expressed *SCGB1B2P*.

All VECs expressed the canonic markers *PECAM1* and *VWF* (Fig 1, *D*). Further analysis separated VECs into venous/venular, capillary, and arterial/arteriolar origins based on their respective expression of *ACKR1*, *GPIHBP1*, and *HEY1* lineage markers (Fig 2, *F*). Capillary VECs abundantly expressed genes involved in fatty acid transport (*CD36* and *FABP4*) (see Fig E3, *F*). Arterial/arteriolar VECs expressed regulators of lymphatic vessel migration and formation (*SEMA3G* and *CXCL12*) and ion exchangers (*SLC9A3R2*, *SLC12A2*, *SLC6A6*, and *ATP13A3*). An additional cluster of venous/venular VECs expressed *NR2F2*, *SELP*, and *CCL23*, likely reflecting a state of vascular inflammation. LECs did not subcluster further.

Macrophages and DCs separated into 1 macrophage and 2 DC (type A DC and type B DC) populations (Fig 2, *G* and see Fig E3, *G*). Macrophages were identified by expression of *RNASE1*, *CD68*, and *SEPP1*. Although both DC clusters expressed *CD1C*, type A DCs were characterized by higher expression of *CD1A* (a Langerhans cell [LC] marker) and *MRC1/CD206* (a marker of immature and inflammatory DCs).[24]

The T cells split into 6 clusters, namely, main T cells, inflammatory T cells, $CD40LG^{+}$ cells, $CD84^{+}$ cells, $CCR6^{+}$ cells, and natural killer T cells (Fig 2, *H* and Fig E3, *H*). Inflammatory T cells were distinguished by high expression of the AD-related cytokine *CSF2*,[25] but also by abundantly expressed type 2 cytokine *IL13*, type 22 cytokine *IL22*, *TNFRSF4/OX40*, and *TNFSF14/LIGHT*, likely representing activated and polarized T cells. The $CD40LG^{+}$, $CD84^{+}$, and $CCR6^{+}$ subgroups likely represent T cells with specialized roles in mediating B-cell activation/class switching, immune regulation via formation of hemophilic dimers,[26] and recruitment

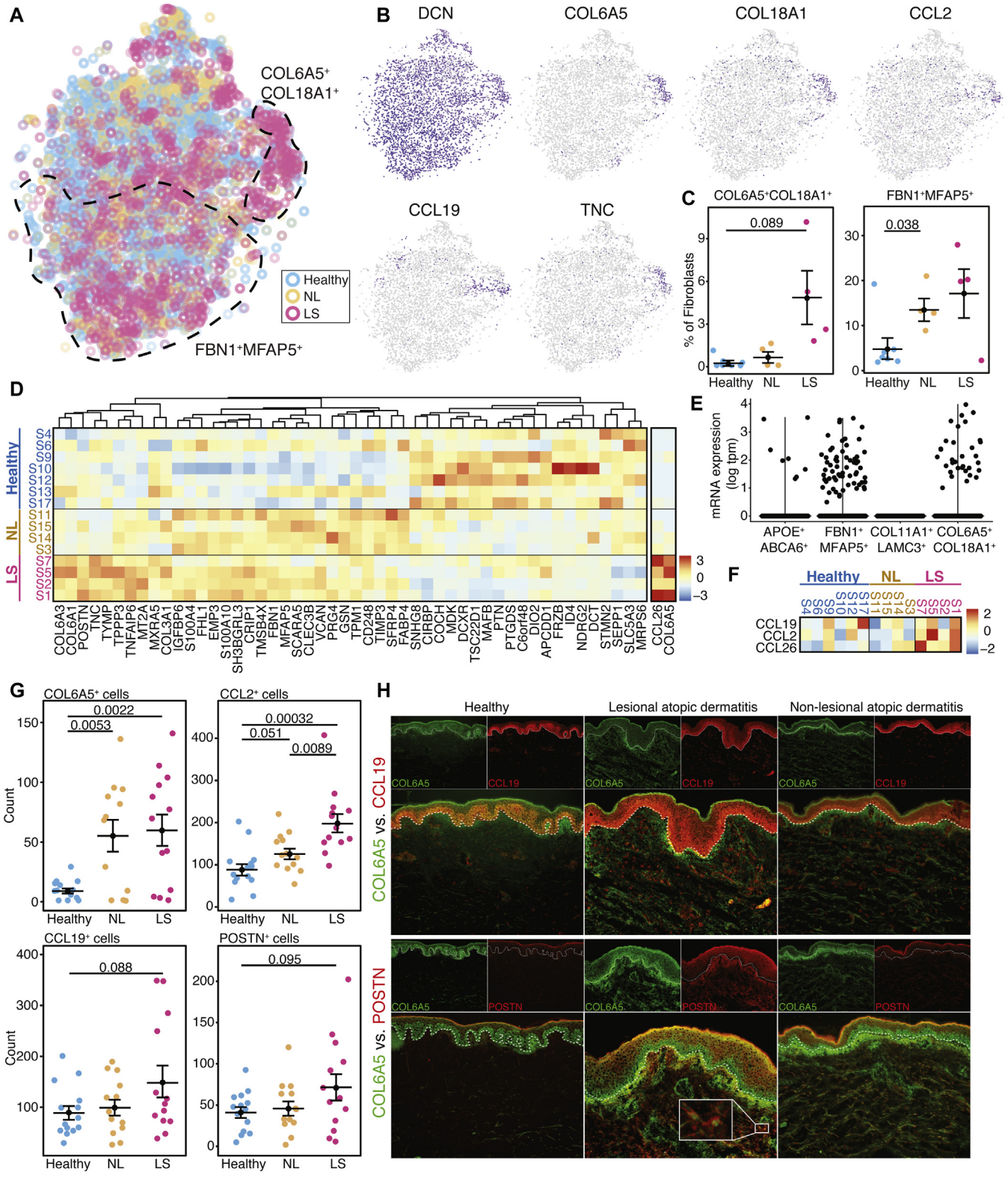

FIG 3. Novel fibroblast subpopulation in lesional AD. **A,** t-Distributed stochastic neighbor embedding plot of combined fibroblast cells, color-coded by tissue type/condition (healthy, nonlesional [NL] AD, and [LS] AD), with the *COL6A5*$^{+}$*COL18A1*$^{+}$ and *FBN1*$^{+}$*MFAP5*$^{+}$ fibroblast clusters delineated by a dotted black line. **B,** Feature plots displaying expression of specific markers among the set of all fibroblasts: *DCN*, *COL6A5*, *COL18A1*, *CCL2*, *CCL19*, and *TNC*. **C,** Frequencies of *COL6A5*$^{+}$*COL18A1*$^{+}$ and *MFAP5*$^{+}$*FBN1*$^{+}$ fibroblasts, as a proportion of all fibroblasts, with pairwise comparisons (with accompanying *P* values with *P* less than .1) among disease conditions. **D,** Unsupervised clustering heatmap showing relative expression (*z* score) levels of the top 50 most abundantly and differentially expressed genes in fibroblasts,

of T_H17 and regulatory T cells, respectively. Finally, natural killer T cells not only expressed *CD3D* but also expressed *NKG7*, *GZMA*, and *GZMK*, highlighting their cytotoxic nature.

To assess the quality of cells from cryopreserved versus fresh samples, an additional fresh biopsy specimen was taken from a healthy volunteer, and subjected to the same analysis, revealing a cell type landscape that overwhelmingly consisted of keratinocytes (92% of all cells) (see Fig E4 in this article's Online Repository at www.jacionline.org). In the fresh healthy sample, 145 FBs and 42 VECs were captured from a total of 4161 cells. In contrast, averaging together all cryopreserved healthy samples, 744 FBs and 821 VECs were captured from a comparable total of 3174 cells.

Novel inflammatory *COL6A5*$^+$*COL18A1*$^+$ fibroblast subpopulation in AD lesions

Most clusters, including fibroblasts, were distributed among all conditions (see Fig E5 in this article's Online Repository at www.jacionline.org). However, *COL6A5*$^+$*COL18A1*$^+$ FBs primarily comprised lesional AD cells (Fig 3, *A*). These FBs expressed inflammatory cytokines (*CCL2*, *CCL19*, and *IL32)* and extracellular matrix (ECM) products that are induced by type 2 inflammation (*POSTN*, *TNC*, and *VCAM1*) (Fig 3, *B* and see Table E2).[27-30] All lesional AD samples showed expansion of *COL6A5*$^+$*COL18A1*$^+$ FBs (Fig 3, *C*), which were not reported by previous studies on healthy fibroblasts (see Fig E6 in this article's Online Repository at www.jacionline.org).[13,14] *MFAP5*$^+$*FBN1*$^+$ FBs were expanded in both lesional and nonlesional skin of patients with AD compared with in healthy skin (Fig 3, *C*).

DEG analysis of FBs demonstrated that *POSTN*, S100 genes (*S100A10* and *S100A11*) and *CRIP1* (a zinc finger suggested to induce type 2 cytokine production in model systems[31]) were upregulated, whereas *PTGDS* (a negative regulator of cell migration/invasion and platelet aggregation) was downregulated, in lesional and/or nonlesional AD versus controls (Fig 3, *D* and see also Table E3 in the Online Repository available at www.jacionline.org).[32] *CCL26*, which is perhaps the best marker of response to type 2 targeting by dupilumab,[33] was highly expressed by lesional AD FBs, primarily in *COL6A5*$^+$*COL18A1*$^+$ and *MFAP5*$^+$*FBN1*$^+$ FBs (Fig 3, *D* and *E*). Like FBs, lesional pericytes highly expressed *CCL2*, *CCL19*, and *CCL26* (Fig 3, *F*).

To validate and determine the anatomic location of these *COL6A5*$^+$*COL18A1*$^+$ FBs, we performed immunohistochemistry staining with cell counts for representative markers (Fig 3, *G* and see Fig E7, *A* in this article's Online Repository at www.jacionline.org). *COL6A5*$^+$ cells were significantly increased in both lesional and nonlesional AD versus controls, most prominently in the upper dermis near the dermal-epidermal junction. Compared with nonlesional skin and controls, AD lesions showed increased infiltration of *CCL2*$^+$ cells, with similar trends for *CCL19* and *POSTN*. Immunofluorescence staining further confirmed *COL6A5*$^+$*CCL19*$^+$ and *COL6A5*$^+$*POSTN*$^+$ double staining in the upper dermis of AD lesions, likely by fibroblast cells (Fig 3, *H*). *COL6A5*$^+$ and *CCL19*$^+$ cells were juxtaposed to *CD3*$^+$ T cells, further supporting a role for these inflammatory FBs in T-cell recruitment and organization (see Fig E7, *B*).

Compositional differences and differentially expressed genes in keratinocytes and other nonimmune cell types in patients with AD compared with in controls

Select KC subpopulations were further subclustered for more detailed profiling of rare subsets. The *TOP2A*$^+$*UBE2C*$^+$ proliferating KC cluster separated into KC.proliferating.1 (expressing *MGST1*, *APOE*, and *KRT17*) and KC.proliferating.2 (*KRT1* and *CCL27*) (Fig 4, *A*). KC.proliferating.1, likely rapidly dividing cells in the hair follicle, contained mostly healthy cells, whereas KC.proliferating.2 overwhelmingly comprised lesional AD cells. Suprabasal keratinocytes resolved into 2 *KRT1*$^+$*KRT10*$^+$ subgroups, 1 of which was predominated by lesional AD cells and expressed keratins enriched in hyperproliferative and wound healing states (*KRT6*, *KRT6A*, and *KRT16*),[34] consistent with epidermal hyperplasia (Fig 4, *B*). Accordingly, lesional AD samples demonstrated increased proportions of *KRT1*$^+$*KRT10*$^+$ and *KRT6A*$^+$*KRT16*$^+$ keratinocytes compared with controls (Fig 4, *C*).

This marked epidermal hyperplasia in lesional AD keratinocytes coincided with increased expression of genes associated with epidermal proliferation, including S100 (*S100A7*, *S100A8*, and *S100A9*) and protease inhibitor (*SERPINB4*) genes (Fig 4, *D* and see Table E3), consistent with the results of previous bulk RNA sequencing.[10] The type 2 chemokine *CCL2* was significantly upregulated in lesional AD versus in controls. *CCL27* (which is required for T-cell recruitment and shown to cause allergen-specific skin inflammation[35]) and *AQP3* (a water channel component associated with KC proliferation and transepidermal water loss[36]) were increased in lesional AD keratinocytes and moderately increased in nonlesional AD keratinocytes. Whereas lesional AD increases in *CCL27* were seen in both basal and suprabasal keratinocytes, *CCL2* and also proinflammatory cytokine *IL32* were increased only in basal keratinocytes and *KRT16*, *AQP3*, and S100s (*S100A2* and *S100A10*) were increased only in suprabasal keratinocytes (Fig 4, *E* and *F* and see Table E3). Pathway enrichment analysis performed with use of the DAVID functional annotation tool[37] showed lesional AD keratinocytes with enrichment of terms

as determined by using criteria log fold change greater than 1 and a false discovery rate less than 0.05, calculated on samples with more than 50 fibroblasts. **E,** Violin plots showing *CCL26* mRNA expression, written as log transcripts per kilobase million, within fibroblast subpopulations. **F,** Heatmap showing relative expression (*z* score) levels of *CCL19*, *CCL2*, and *CCL26* in pericytes, calculated on samples with more than 10 pericytes. **G,** Cell counts for *COL6A5*, *CCL2*, *CCL19*, and *POSTN* in healthy, nonlesional AD, and lesional AD samples with pairwise comparisons and accompanying *P* values with *P* less than .1. **H,** Immunofluorescence staining of *COL6A5* (*green*)/*CCL19* (*red*), *COL6A5* (*green*)/*POSTN* (*red*), and their respective overlays in healthy, lesional AD, and nonlesional AD samples, with the dotted line outlining the dermal-epidermal junction. Zoomed-in insert of *COL6A5*/*POSTN* costaining in individual cells. *DCN*, Decorin; *TNC*, tenascin-C.

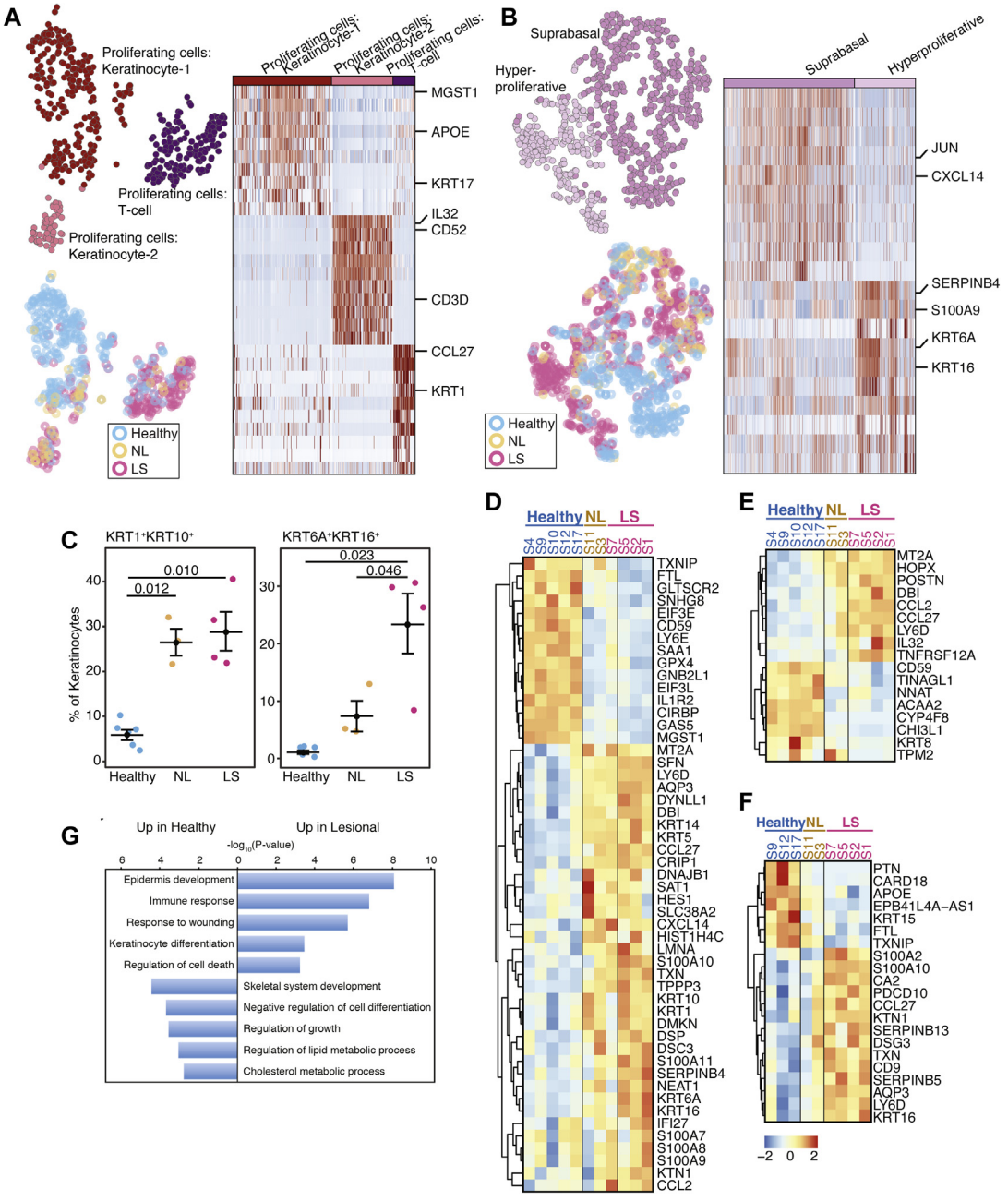

FIG 4. Keratinocyte compositional and gene expression changes in AD. **A,** t-Distributed stochastic neighbor embedding plot of proliferating keratinocytes and T cells, color-coded by cell subpopulation and by disease condition, with an accompanying heatmap of distinct gene signatures (top 10 differentially expressed genes; Wilcoxon rank sum test). **B,** t-Distributed stochastic neighbor embedding plot of suprabasal keratinocytes, color-coded by cell subpopulation and by disease condition, with an accompanying heatmap of distinct gene signatures (top 10 differentially expressed genes; Wilcoxon rank sum test). **C,** Frequencies of *KRT1*$^{+}$*KRT10*$^{+}$ and *KRT16*$^{+}$*KRT6A*$^{+}$ keratinocytes, as a percentage of all keratinocytes, with pairwise comparisons (and accompanying *P* values with *P* less than .1) among disease conditions (healthy, nonlesional [NL] AD, and lesional [LS] AD). **D,** Unsupervised clustering heatmap showing relative expression (*z* score) levels of the top 50 most abundantly and differentially expressed genes in keratinocytes, as determined by using criteria log fold change greater than 1 and FDR less than 0.05, calculated on samples with more than 50 keratinocytes. **E,** Unsupervised clustering heatmap showing relative expression (*z* score) levels of differentially expressed genes in basal keratinocytes, as determined by using criteria log fold change greater than 1 and FDR less than 0.05, calculated on samples with more than 10 basal keratinocytes. **F,** Unsupervised clustering heatmap showing relative expression (*z* score) levels of differentially expressed genes in suprabasal keratinocytes using criterion log fold change greater than 1 and FDR less than 0.05, calculated on samples with more than 10 suprabasal keratinocytes. **G,** Gene ontology terms enriched in lesional versus in healthy keratinocytes, as obtained by using DAVID. The top 5 most upregulated and downregulated gene sets in lesional AD versus controls (with the lowest *P* value and composed of more than 3 genes) are depicted as bar plots displaying $-\log_{10}$ (*P* value). *LS*, Lesional; *NL*, nonlesional.

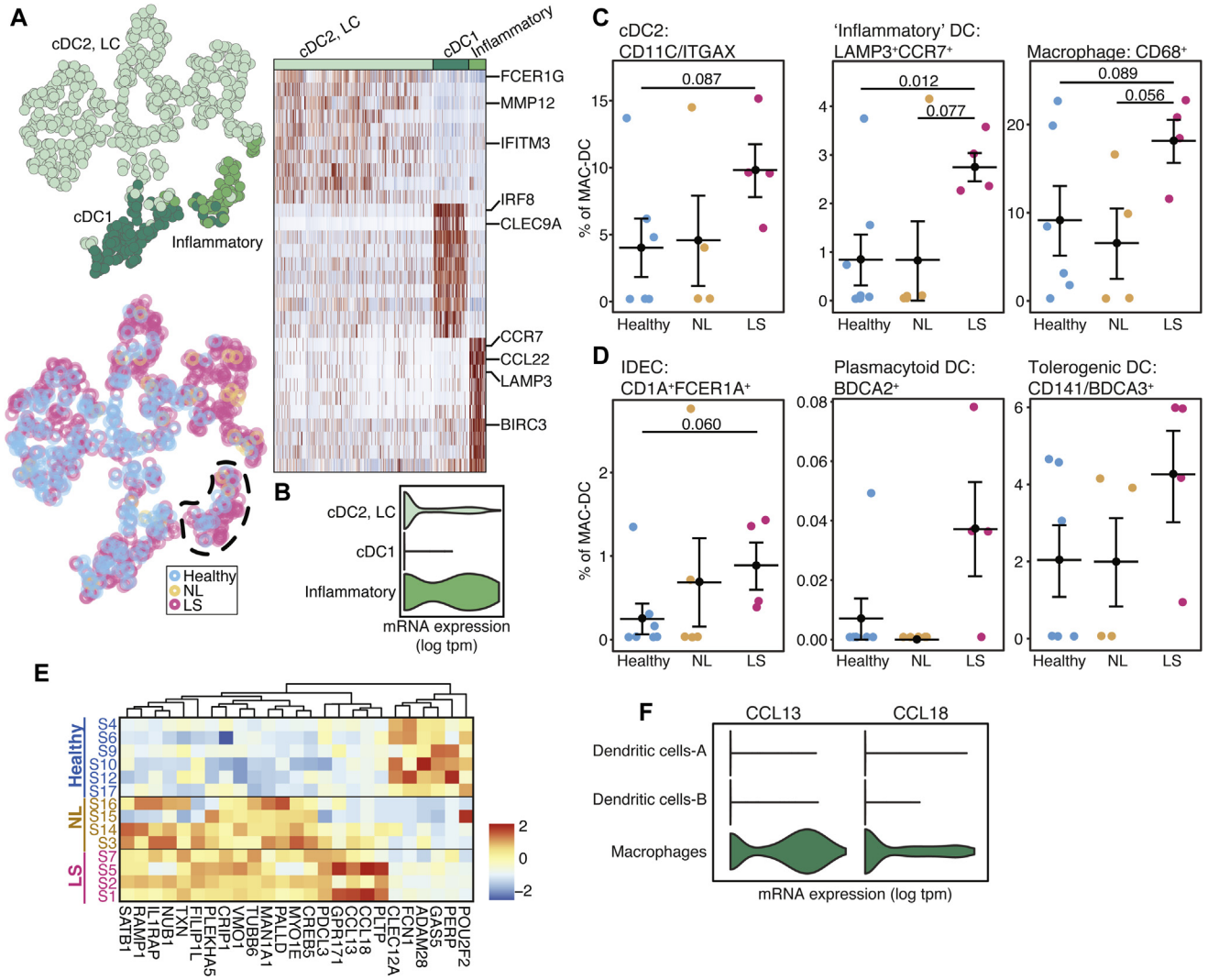

FIG 5. Compositional and gene expression changes among macrophages and DCs in AD. **A,** t-Distributed stochastic neighbor embedding plot of DCs, color-coded by cell subpopulation and by disease condition, with an accompanying heatmap of distinct gene signatures (top 10 differentially expressed genes, Wilcoxon rank sum test). **B,** Violin plot showing *CCL17* mRNA expression, written as log transcripts per kilobase million (tpm) value, within DC subpopulations. **C** and **D,** Frequencies of DC and macrophage subsets as a percentage of all macrophages and DCs in the sample, with pairwise comparisons among disease conditions (healthy, nonlesional [NL] AD, and lesional [LS] AD), as obtained from subclustering **(C)** and from previously defined lineage markers **(D)**. **E,** Unsupervised clustering heatmap showing relative expression (*z* score) levels of differentially expressed genes in macrophages and DCs, as determined by using criteria log fold change greater than 1 and FDR less than 0.05, calculated on samples with more than 10 macrophages and DCs. **F,** Violin plot showing *CCL13* and *CCL18* mRNA expression, written as log tpm within macrophage/DC subpopulations. *IDEC,* Inflammatory dendritic epidermal cell; *MAC,* macrophage.

such as epidermis development, immune response, and response to wound healing, whereas healthy keratinocytes were enriched in negative regulation of cell differentiation, regulation of growth, and regulation of lipid metabolic process (Fig 4, *G*).

Identification and expansion of *LAMP3*$^{+}$*CCR7*$^{+}$ and other DC subsets in AD

The major DC subsets in healthy human skin include epidermal LCs and dermal conventional DCs (cDCs), further subdivided into type 1 (cDC1) and type 2 (cDC2) subsets.[38] Type A and B DCs were combined and further resolved into 3 clusters (Fig 5, *A*). The largest subgroup had the highest expression of *CD1C* and also uniquely expressed *CD11C*/*ITGAX* and *CD207*/langerin, likely corresponding to a combined cDC2 and LC cluster. The second cluster highly expressed the cDC1 markers *CLEC9A* and *IRF8*. Finally, a small but important population expressing *LAMP3* (a marker of mature DCs consisting primarily of lesional AD cells) was distinguished by robust expression of the type 2 chemokines *CCL17* and *CCL22* and expression of the *CCL19* receptor *CCR7* (Fig 5, *A* and *B*). cDC2 (*CD11C*$^{+}$) and *LAMP3*-$^{+}$*CCR7*$^{+}$ DCs, as well as *CD68*$^{+}$ macrophages were expanded in lesional AD versus controls (Fig 5, *C*). Proportional frequencies

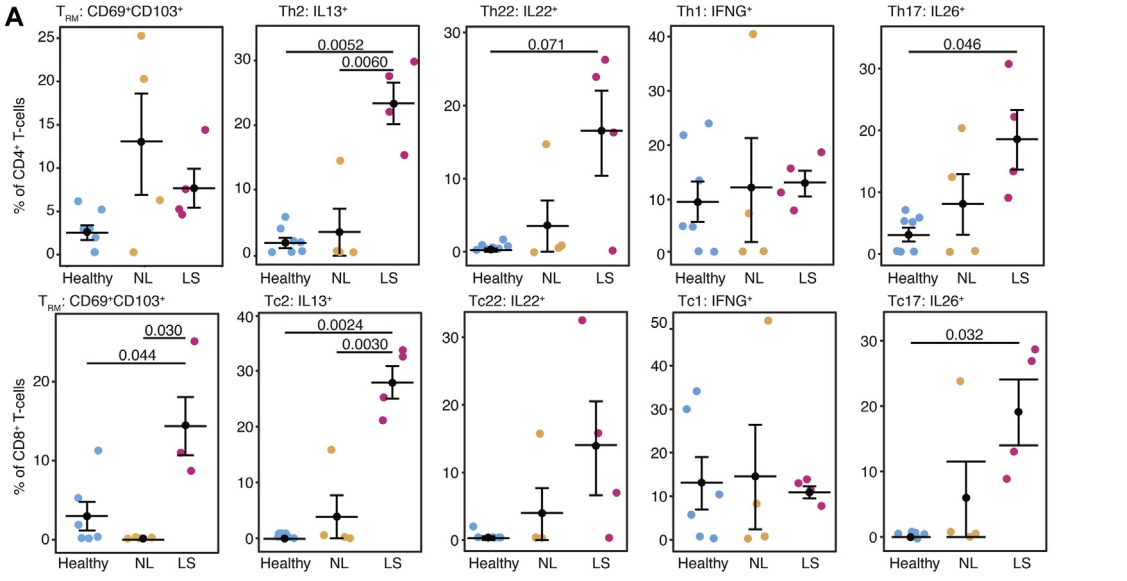

C

All	Healthy	NL	LS
IL13+	2.66	11.94	22.91
IL22+	0.95	12.69	20.08
IL26+	4.38	11.94	17.63
IFNG+	5.07	5.97	5.92
IL13+/IFNG+	0.53	2.00	3.87
IL22+/IFNG+	0.19	2.13	3.39
IL26+/IFNG+	0.86	2.00	2.98

CD4+	Healthy	NL	LS
Th2	3.42	12.73	19.10
Th22	0.99	12.73	16.58
Th17	4.38	11.82	16.40
Th1	2.76	2.73	3.42
Th2/Th1	1.24	4.67	5.58
Th22/Th1	0.36	4.67	4.84
Th17/Th1	1.88	4.33	4.79

CD8+	Healthy	NL	LS
Tc2	0.00	11.76	25.41
Tc22	1.18	11.76	17.21
Tc17	0.00	17.65	15.57
Tc1	9.41	11.76	9.02
Tc2/Tc1	0.00	1.00	2.82
Tc22/Tc1	0.13	1.00	1.91
Tc17/Tc1	0.00	1.50	1.73

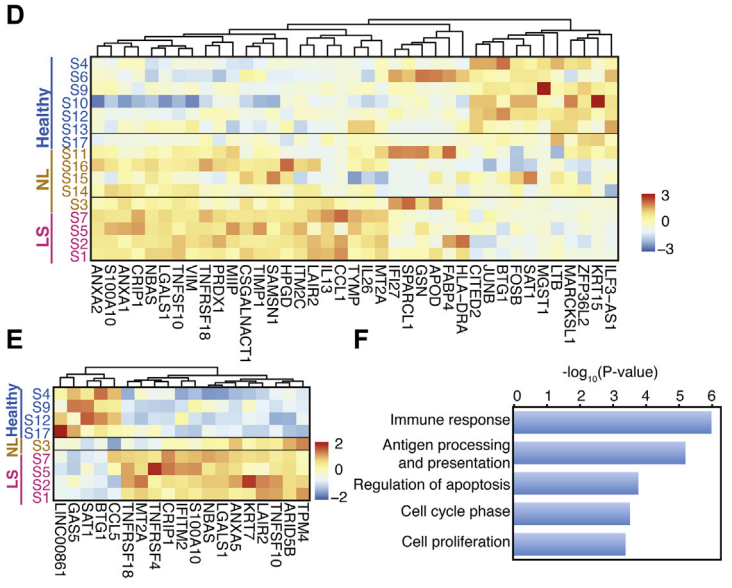

FIG 6. Compositional and gene expression changes among T cells in AD. **A,** Frequencies of tissue-TRM cells (*CD69*$^+$*CD103*$^+$), T_H2/T_C2 cells (*IL13*$^+$), T_H22/T_C22 cells (*IL22*$^+$), T_H1/Tc1 cells (*IFNG*$^+$), and T_H17/Tc17 cells (*IL26*$^+$), as the percentage of all T cells, within both *CD4*$^+$ and *CD8*$^+$ subsets, with pairwise comparisons (and accompanying *P* values with *P* less than .1) among disease conditions (healthy, nonlesional [NL] AD, lesional [LS] AD). **B,** Immunofluorescence staining of tissue T_{RM} T-cell markers *CD69* (*red*), *CD103* (*green*), and *CD69*/*CD103* overlay in healthy, nonlesional AD, and lesional AD sample, with dotted line outlining the dermal-epidermal junction. **C,** Table of percentages of *IL13*$^+$, *IL22*$^+$, *IL26*$^+$, and *IFNG*$^+$ cells, as a percentage of all T cells, all *CD4*$^+$ cells, and all *CD8*$^+$ cells, as well as *IL13*$^+$/*IFNG*$^+$, *IL22*$^+$/*IFNG*$^+$, and *IL26*$^+$/*IFNG*$^+$ ratios for each condition (healthy, nonlesional AD, and lesional AD). **D,** Unsupervised clustering heatmap showing relative expression (*z* score) levels of the top 50 most abundantly and differentially expressed genes in T cells using criteria log fold change greater than 1 and FDR less than 0.05, calculated on samples with more than 50 T cells. **E,** Unsupervised clustering heatmap showing relative expression (*z* score) levels of differentially expressed genes in *CD4*$^+$ T cells using criteria log fold change more than 1 and FDR less than 0.05. **F,** Gene ontology terms enriched in lesional AD versus healthy T cells, as obtained by using DAVID. The 5 gene sets with the lowest *P* value and composed of more than 3 genes are depicted as bar plots displaying $-\log_{10}$ (*P* value).

of other DC subsets that were previously found in the skin[39-42] but were not resolvable by clustering, likely because of their rarity, were calculated on the basis of characteristic markers (Fig 5, *D*). Inflammatory dendritic epidermal cells, which are *CD1A*$^+$*FCER1A*$^+$ and highly specific to AD,[41] were expanded in lesional AD relative to other DC subsets. *BDCA3*$^+$ DCs, which are tolerogenic and promote regulatory T-cell differentiation,[39] and *BDCA2*$^+$ plasmacytoid DCs, were also slightly higher in lesional AD than in controls (Fig 5, *D*). Lesional AD macrophages and DCs showed increases in type 2 chemokines *CCL13* and *CCL18*, which are expressed by macrophages (Fig 5, *E* and *F*).

Expansion of CD8$^+$ tissue T_{RM}, T_H2/T_C2, and T_H22 cells in AD lesions

Because mitotic cells clustered together on the basis of characteristic markers (eg, *UBE2C* and *TOP2A*), the proliferating KC subpopulation also featured a proliferating TC cluster dominated by lesional AD cells (Fig 4, *A*). Resident memory T cells (T_{RM}), which express *CD69* and/or *CD103*,[43,44] were significantly expanded in lesional AD skin compared with in healthy and nonlesional AD skin, only within the CD8$^+$ subset (Fig 6, *A*). Immunofluorescence costaining also showed relative expansion of *CD69*$^+$*CD103*$^+$ cells, especially in the epidermis, for lesional AD (45 cells [24 in epidermis and 21 in dermis]) compared with for nonlesional AD (17 cells [13 in epidermis and 4 in dermis]) and controls (1 cell [0 in epidermis and 1 in dermis]) (Fig 6, *B*). The frequency of *CD4*$^+$/*CD8*$^+$ type 2 (*IL13*$^+$) and type 17 (*IL26*$^+$) cells was significantly increased in lesional AD compared with in both healthy and nonlesional AD samples (Fig 6, *A*). Levels of type 22 (*IL22*$^+$) T cells were also expanded in lesional AD, more in the *CD4*$^+$ subset, whereas levels of type 1 (*IFNG*$^+$) T cells were comparable in patients with AD and controls.

The proportion of T cells that were type 2, type 22, or type 17 was markedly higher (from 2.98- to 3.87-fold) compared with the proportion of type 1 in lesional AD (type 2, 22.9%; type 22, 20.1%; type 17, 17.6%; and type 1, 5.9%), with a similar trend for nonlesional AD (type 2, 11.9%; type 22, 12.7%; type 17, 11.9; and type 1, 6.0%), whereas healthy controls showed the reverse trend, with type 1 cells outnumbering both type 2 and type 22 cells (type 2, 2.7%; type 22, 0.95%; type 17, 4.4%; and type 1, 5.1%) (Fig 6, *C*). Similar trends were observed within the *CD4*$^+$ and *CD8*$^+$ subsets. A higher percentage of proliferating *UBE2C*$^+$*TOP2A*$^+$ lesional AD T cells were identified to be *IL13*$^+$ (33.9%), *IL22*$^+$ (20.7%), or *IL26*$^+$ (38.0%) compared with *IFNG*$^+$ (8.3%), suggesting active expansion of memory/effector type 2, 22, and 17 cells in AD lesions.

Lesional T cells showed elevated expression of T-cell activation and monocyte chemotactic chemokine *CCL1*, type 2/type 17 cytokines *IL13* and *IL26*, and annexin genes (*ANXA1* and *ANXA2*) that have various roles in regulating inflammation, wound healing, and apoptosis (Fig 6, *D* and see Table E3). Taking only *CD4*$^+$ cells, lesional AD showed additional upregulation of *TNFRSF4/OX40* (which promotes type 2 responses and may be a therapeutic target in AD[45]), *TNFSF10/TRAIL* (a TC activation and proapoptotic marker), *TNFRSF18* (which may function in self-tolerance[46]), and *IFITM2* (an interferon-induced gene) (Fig 6, *E*). Pathway enrichment analysis revealed enrichment of immune response, antigen processing and presentation, and regulation of apoptosis in lesional AD T cells (Fig 6, *F*).

Cell-cell communication in AD

To investigate potential intercellular communications among cell types, we visualized average expression levels of the most abundant (>3 TPM) ligands and their cognate receptors (>0.4 TPM) that were differentially expressed in lesional AD versus in controls (Fig 7). In AD lesions, the interaction between *CCL19* produced by the inflammatory *COL6A5*$^+$*COL18A1*$^+$ FB subpopulation and *CCR7* on T cells and macrophages-DCs (particularly *LAMP3*$^+$ DCs), is critical for regulating lymphoid cell organization and trafficking. The type 2 chemokine *CCL2* was abundantly expressed by inflammatory FBs and keratinocytes, whereas its receptors *CCR1* and *CCR2* were expressed on macrophages and DCs. Lesional T cells highly expressed the key type 2 cytokine *IL13*, signaling via *IL4R* and *IL13RA1* on FBs and on pericytes and vSMCs. *CCL27* was upregulated in lesional keratinocytes, which is suggestive of signaling via *CCR10* on TCs, highlighting communication between primarily "nonimmune" (eg, FBs, keratinocytes) and immune cells.

DISCUSSION

We have presented what, to our knowledge, is the first comprehensive, high-resolution, single-cell transcriptomic analysis of all cell types and expression programs from patients with AD compared with from healthy controls. Our atlas of combined AD skin and healthy skin comprises 10 broad cell types. Through high-resolution subclustering, we identified rare subpopulations that were unreported in previous scRNA-seq skin studies.[12-15] Examples include clear and dark cells in the secretory coil of sweat glands, and gap junctions and ATPase channels in keratinocytes, which concur with but add further resolution to the "channel keratinocytes" identified by Cheng et al.[12]

Previous bulk RNA sequencing and microarray transcriptomic studies on AD skin revealed dysregulation of inflammatory (*IL13* and *CCL2*) and barrier (*KRT16, S100A8*, and *S100A9*) genes,[10,47-49] but many markers, including those representing polar T_H cytokines, often remain masked in whole-skin transcriptomic analyses.[10,48,49] Here, we have provided cell type–level resolution of primary cytokines associated with AD (eg, *IL13*, *IL22*) and have identified novel *COL6A5*$^+$*COL18A1*$^+$ FBs that produce key molecules driving AD inflammation (eg, *CCL2*, *CCL19*, *POSTN*, and *TNC*).

This FB cluster, which is unique to AD lesions, harbors a distinct collagen expression pattern, with high levels of *COL6A5* and *COL18A1*. Whereas we localized *COL6A5* to the papillary dermis, and particularly near the dermal-epidermal junction, which is consistent with previous reports,[13,50,51] we have now also demonstrated marked *COL6A5* expansion in AD lesions. *COL6A5* has been identified as an AD susceptibility gene,[50] although these studies were inconsistent[52-56] and without a clear mechanism. The pathogenic role of *COL6A5* in AD may be due to the formation of unstable heterotrimers, leading to aberrant fibroblast adhesion, collagen synthesis and metabolism, and barrier disruption.[51] *COL6A5* is also found in other sites of allergic disorders (eg, skin, lung, small intestine, colon), and may promote

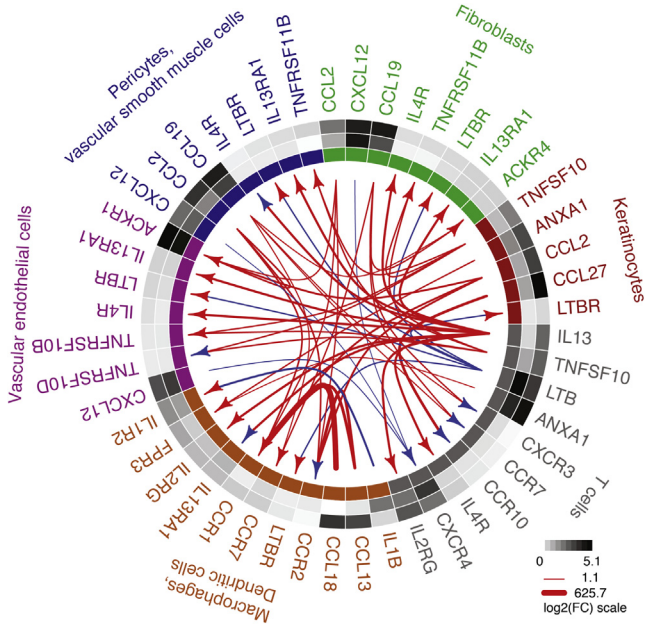

FIG 7. Interactions between differentially expressed ligands and receptors in lesional AD versus healthy subjects. *Arrows* are pointing to the receptors, with the size of the arrow stem proportionate to expression levels of ligands in log-scale. Cutoffs were >3 transcripts per kilobase million for ligands and >0.4 transcripts per kilobase million for receptors. Cell types were only included if they comprised >100 cells in more than 50% of samples.

allergen sensitization and inflammation by regulating LCs and T cells.[50] *COL18A1*/endostatin potently inhibits angiogenesis and binds to several other ECM components,[57] and it may similarly contribute to ECM disorganization and instability in AD.

Along with promoting barrier and structural instability, these FBs also have an inflammatory role. They highly express *CCL2*, implicating a function in type 2 cell polarization,[58] and *CCL19*, which is important for lymphocyte recirculation, homing, and migration to secondary lymphoid organs.[59] The cross talk between fibroblasts and DCs in AD is supported by the lesional skin enrichment of mature (*LAMP3*$^+$) DCs expressing *CCR7*, the receptor for *CCL19*, and type 2 chemokines *CCL17* and *CCL22*, suggesting that FBs interact with macrophages and DCs to facilitate T-cell trafficking, lymphoid tissue organization, and type 2 cell recruitment. These FBs also express *POSTN* and *TNC*, which encode ECM proteins that are induced by the defining and profibrotic type 2 cytokines *IL4* and *IL13*,[60,61] which are upregulated in AD,[28,62] and may further propagate type 2 inflammation and fibrotic remodeling in a vicious inflammatory cycle. These FBs may also play a role in fibrotic skin conditions that also have an inflammatory (type 2) component (eg, scleroderma, keloids).[63,64] Recent studies describing stromal cells in lung and other tissues that promote type 2 responses (eg, *IL33*, *TSLP*, *CCL18*) and are inducible by *IL4*/*IL13* further support a role for fibroblasts in mediating type 2 immunity and atopy across organ systems.[63,65-67]

These inflammatory *COL6A5*$^+$*COL18A1*$^+$ FBs were unrecognized by prior single-cell studies on healthy dermal fibroblasts.[13,14] Whereas our overall FB composition, including *COL11A1*$^+$ FBs, agreed with these studies, we report different gene expression patterns in the major clusters, likely reflecting the plasticity within fibroblasts and/or transcription responses to increased inflammatory cytokines in AD. For example, whereas Tabib et al found that *FMO1*$^+$ FBs constituted a major population, we found very low levels of *FMO1* in FBs.[14] Interestingly, Philippeos et al did report an FB cluster that expressed *COL6A5* but lacked other proinflammatory properties, and they instead attributed this cluster to general papillary fibroblasts.[13]

ScRNA-seq provides a direct, reliable, and more detailed characterization of immune subsets in AD, compared with indirect cell origin inference by the open chromatin analysis used in bulk transcriptomic studies.[47] For example, actively proliferating *UBE2C*$^+$*TOP2A*$^+$ type 2/type 22 T cells were expanded in lesional AD and were either absent or less abundant in nonlesional and healthy samples. T_{RM} cells, which are crucial to cutaneous homeostasis in healthy skin but become aberrant in certain autoimmune and inflammatory diseases such as psoriasis,[43,44,68] were not previously reported in AD. Here, we found that T_{RM} cells were expanded in AD lesions. Whether T_{RM} expansion constitutes a homeostatic response to inflammation or an active contributor to AD pathogenesis is unclear. In future studies, to fully understand the role of T_{RM} persistence in disease recurrence, as is seen in psoriasis,[30,31,47] it would be beneficial to evaluate T_{RM} expression in resolved AD lesions after successful treatment.

Although flow cytometry studies showed increases in type 2/type 22 populations in AD lesions,[69,70] the current study shows preferential activation of T_H2/T_C2 and T_H22 TCs, as compared with in controls, in which type 1 T cells are preferentially expanded. This study has been able to define transcriptionally activated cells that are producing polar T-cell cytokines, without the artificial activation stimulus required for flow cytometric studies. Respective interactions between *CCL2* and *CCL27* in keratinocytes and *CCR2* and *CCR10* on T cells likely promote type 2/type 22 differentiation, suggesting that keratinocytes are part of a "feed forward" inflammatory response by producing chemokines that promote AD-related immune abnormalities. In turn, type 22 T cells mediate many of the compositional or gene expression changes observed in keratinocytes, including S100 gene production and epidermal hyperplasia,[70] as reflected by enrichment of hyperproliferative (*KRT6A* and *KRT16*) and early differentiation (*KRT1* and *KRT10*) keratins.

This study has some limitations. We were unable to recover certain KC populations, such as stratum corneum cells expressing late differentiation markers (eg, *FLG*), which may possibly be attributed to cell damage induced by cryopreservation and/or cell type sensitivity to enzymatic digestion. However, we still characterized several keratinocyte subpopulations corresponding to multiple anatomic compartments of the epidermis, aligning with previously published scRNA-seq on keratinocyte populations in healthy fresh tissue.[12] Our data suggest that cryopreservation may even improve recovery of dermal cell populations such as FBs and VECs. Second, our study involved a limited number of samples, restricting our ability to use graph-based clustering to resolve certain cell types, such as DCs or *CD4*$^+$ versus *CD8*$^+$ TCs, which is an issue that is shared by other scRNA-seq skin studies[12] and thus required us to identify these groups by other means such as automatic cell annotation tools. Our findings require validation with a larger cohort.

This is the first detailed single-cell transcriptomic profiling of lesional and nonlesional skin from patients with AD compared with from healthy controls, providing new insights into the

complex interplay of cell types and gene expression changes involved in AD pathogenesis. Our study demonstrates the utility of scRNA-seq on small cryopreserved skin biopsy specimens to detect disease-related compositional and gene expression characteristics in AD and other inflammatory skin diseases at steady states or in response to therapeutics during clinical trials. We are providing a detailed molecular map of various cell types and potential interactions involved in orchestrating AD-specific inflammation and barrier alterations. This previously unrecognized fibroblast cluster with inflammatory properties is of particular interest, because although immune and barrier abnormalities are established in AD, the role of ECM cells and genes in these processes are largely unknown. These fibroblasts may signal to immune cells to mediate ECM breakdown, fibrotic remodeling, and T-cell recruitment and polarization, requiring validation in future studies. These cells and their respective products are potential future therapeutic targets in AD and other inflammatory or fibrotic skin diseases.

We acknowledge expert support by the members of the Rockefeller University Genomics Resource Center and the Epigenomics Core facility of Weil Cornell Medicine. The authors thank Arlene Hurley, NP, and the Research Facilitation Office staff at Rockefeller University for regulatory and administrative assistance supported in part by grant UL1TR001866 from the National Center for Advancing Translational Sciences, National Institutes of Health, Clinical and Translational Science Award program. We also thank Qiaolin Deng (Karolinska Institutet) for editorial comments, and we thank Seulah Choi (Mount Sinai) for her assistance with editing figures.

Clinical implications: This is the first single-cell transcriptome defining constitutive cytokine activation by fibroblasts and polarized T cells in AD skin, suggesting these inflammatory products as potential therapeutic targets. Single-cell profiling may be used to evaluate therapeutic responses in clinical trials for inflammatory skin diseases.

REFERENCES

1. Chiesa Fuxench ZC, Block JK, Boguniewicz M, Boyle J, Fonacier L, Gelfand JM, et al. Atopic dermatitis in america study: a cross-sectional study examining the prevalence and disease burden of atopic dermatitis in the US adult population. J Invest Dermatol 2019;139:583-90.
2. Silverberg JI, Simpson EL. Association between severe eczema in children and multiple comorbid conditions and increased healthcare utilization. Pediatr Allergy Immunol 2013;24:476-86.
3. Brandt EB, Sivaprasad U. Th2 cytokines and atopic dermatitis. J Clin Cell Immunol 2011;2.
4. Esaki H, Ewald DA, Ungar B, Rozenblit M, Zheng X, Xu H, et al. Identification of novel immune and barrier genes in atopic dermatitis by laser capture micro-dissection. J Allergy Clin Immunol 2015;135:153-63.
5. Agrawal R, Woodfolk JA. Skin barrier defects in atopic dermatitis. Curr Allergy Asthma Rep 2014;14:433.
6. Noda S, Suarez-Farinas M, Ungar B, Kim SJ, de Guzman Strong C, Xu H, et al. The Asian atopic dermatitis phenotype combines features of atopic dermatitis and psoriasis with increased TH17 polarization. J Allergy Clin Immunol 2015;136:1254-64.
7. Sanyal RD, Pavel AB, Glickman J, Chan TC, Zheng X, Zhang N, et al. Atopic dermatitis in African American patients is TH2/TH22-skewed with TH1/TH17 attenuation. Ann Allergy Asthma Immunol 2019;122:99-110.
8. Suarez-Farinas M, Dhingra N, Gittler J, Shemer A, Cardinale I, de Guzman Strong C, et al. Intrinsic atopic dermatitis shows similar TH2 and higher TH17 immune activation compared with extrinsic atopic dermatitis. J Allergy Clin Immunol 2013;132:361-70.
9. Suárez-Fariñas M, Tintle SJ, Shemer A, Chiricozzi A, Nograles K, Cardinale I, et al. Nonlesional atopic dermatitis skin is characterized by broad terminal differentiation defects and variable immune abnormalities. J Allergy Clin Immunol 2011;127:954-64.
10. Suarez-Farinas M, Ungar B, Correa da Rosa J, Ewald DA, Rozenblit M, Gonzalez J, et al. RNA sequencing atopic dermatitis transcriptome profiling provides insights into novel disease mechanisms with potential therapeutic implications. J Allergy Clin Immunol 2015;135:1218-27.
11. Nomura I, Gao B, Boguniewicz M, Darst MA, Travers JB, Leung DY. Distinct patterns of gene expression in the skin lesions of atopic dermatitis and psoriasis: a gene microarray analysis. J Allergy Clin Immunol 2003;112:1195-202.
12. Cheng JB, Sedgewick AJ, Finnegan AI, Harirchian P, Lee J, Kwon S, et al. Transcriptional programming of normal and inflamed human epidermis at single-cell resolution. Cell Rep 2018;25:871-83.
13. Philippeos C, Telerman SB, Oules B, Pisco AO, Shaw TJ, Elgueta R, et al. Spatial and single-cell transcriptional profiling identifies functionally distinct human dermal fibroblast subpopulations. J Invest Dermatol 2018;138:811-25.
14. Tabib T, Morse C, Wang T, Chen W, Lafyatis R. SFRP2/DPP4 and FMO1/LSP1 define major fibroblast populations in human skin. J Invest Dermatol 2018;138:802-10.
15. Joost S, Zeisel A, Jacob T, Sun X, La Manno G, Lönnerberg P, et al. Single-cell transcriptomics reveals that differentiation and spatial signatures shape epidermal and hair follicle heterogeneity. Cell Syst 2016;3:221-37.
16. Der E, Suryawanshi H, Morozov P, Kustagi M, Goilav B, Ranabathou S, et al. Tubular cell and keratinocyte single-cell transcriptomics applied to lupus nephritis reveal type I IFN and fibrosis relevant pathways. Nat Immunol 2019.
17. Der E, Ranabothu S, Suryawanshi H, Akat KM, Clancy R, Morozov P, et al. Single cell RNA sequencing to dissect the molecular heterogeneity in lupus nephritis. JCI Insight 2017;2.
18. Mabbott NA, Baillie JK, Brown H, Freeman TC, Hume DA. An expression atlas of human primary cells: inference of gene function from coexpression networks. BMC Genomics 2013;14:632.
19. Pruenster M, Mudde L, Bombosi P, Dimitrova S, Zsak M, Middleton J, et al. The Duffy antigen receptor for chemokines transports chemokines and supports their promigratory activity. Nat Immunol 2009;10:101-8.
20. Zheng GX, Terry JM, Belgrader P, Ryvkin P, Bent ZW, Wilson R, et al. Massively parallel digital transcriptional profiling of single cells. Nat Commun 2017;8:14049.
21. Veniaminova NA, Vagnozzi AN, Kopinke D, Do TT, Murtaugh LC, Maillard I, et al. Keratin 79 identifies a novel population of migratory epithelial cells that initiates hair canal morphogenesis and regeneration. Development 2013;140:4870-80.
22. Hotamisligil GS, Bernlohr DA. Metabolic functions of FABPs–mechanisms and therapeutic implications. Nat Rev Endocrinol 2015;11:592-605.
23. Cui CY, Schlessinger D. Eccrine sweat gland development and sweat secretion. Exp Dermatol 2015;24:644-50.
24. Wollenberg A, Mommaas M, Oppel T, Schottdorf EM, Gunther S, Moderer M. Expression and function of the mannose receptor CD206 on epidermal dendritic cells in inflammatory skin diseases. J Invest Dermatol 2002;118:327-34.
25. Choy DF, Hsu DK, Seshasayee D, Fung MA, Modrusan Z, Martin F, et al. Comparative transcriptomic analyses of atopic dermatitis and psoriasis reveal shared neutrophilic inflammation. J Allergy Clin Immunol 2012;130:1335-43.
26. Lewinsky H, Barak AF, Huber V, Kramer MP, Radomir L, Sever L, et al. CD84 regulates PD-1/PD-L1 expression and function in chronic lymphocytic leukemia. J Clin Invest 2018;128:5465-78.
27. Yeo SY, Lee KW, Shin D, An S, Cho KH, Kim SH. A positive feedback loop bistably activates fibroblasts. Nat Commun 2018;9:3016.
28. Shiraishi H, Masuoka M, Ohta S, Suzuki S, Arima K, Taniguchi K, et al. Periostin contributes to the pathogenesis of atopic dermatitis by inducing TSLP production from keratinocytes. Allergol Int 2012;61:563-72.
29. Masuoka M, Shiraishi H, Ohta S, Suzuki S, Arima K, Aoki S, et al. Periostin promotes chronic allergic inflammation in response to Th2 cytokines. J Clin Invest 2012;122:2590-600.
30. Gao JX, Issekutz AC. Expression of VCAM-1 and VLA-4 dependent T-lymphocyte adhesion to dermal fibroblasts stimulated with proinflammatory cytokines. Immunology 1996;89:375-83.
31. Lanningham-Foster L, Green CL, Langkamp-Henken B, Davis BA, Nguyen KT, Bender BS, et al. Overexpression of CRIP in transgenic mice alters cytokine patterns and the immune response. Am J Physiol Endocrinol Metab 2002;282.
32. Wu CC, Shyu RY, Wang CH, Tsai TC, Wang LK, Chen ML, et al. Involvement of the prostaglandin D2 signal pathway in retinoid-inducible gene 1 (RIG1)-mediated suppression of cell invasion in testis cancer cells. Biochim Biophys Acta 2012;1823:2227-36.
33. Hamilton JD, Suarez-Farinas M, Dhingra N, Cardinale I, Li X, Kostic A, et al. Dupilumab improves the molecular signature in skin of patients with moderate-to-severe atopic dermatitis. J Allergy Clin Immunol 2014;134:1293-300.

34. Lessard JC, Piña-Paz S, Rotty JD, Hickerson RP, Kaspar RL, Balmain A, et al. Keratin 16 regulates innate immunity in response to epidermal barrier breach. Proc Natl Acad Sci U S A 2013;110:19537-42.
35. Homey B, Alenius H, Muller A, Soto H, Bowman EP, Yuan W, et al. CCL27-CCR10 interactions regulate T cell-mediated skin inflammation. Nat Med 2002;8:157-65.
36. Nakahigashi K, Kabashima K, Ikoma A, Verkman AS, Miyachi Y, Hara-Chikuma M. Upregulation of aquaporin-3 is involved in keratinocyte proliferation and epidermal hyperplasia. J Invest Dermatol 2011;131:865-73.
37. Huang da W, Sherman BT, Lempicki RA. Systematic and integrative analysis of large gene lists using DAVID bioinformatics resources. Nat Protoc 2009;4:44-57.
38. Kim TG, Kim SH, Lee MG. The origin of skin dendritic cell network and its role in psoriasis. Int J Mol Sci 2017;19.
39. Chu CC, Ali N, Karagiannis P, Di Meglio P, Skowera A, Napolitano L, et al. Resident CD141 (BDCA3)+ dendritic cells in human skin produce IL-10 and induce regulatory T cells that suppress skin inflammation. J Exp Med 2012;209:935-45.
40. Fujita H, Shemer A, Suarez-Farinas M, Johnson-Huang LM, Tintle S, Cardinale I, et al. Lesional dendritic cells in patients with chronic atopic dermatitis and psoriasis exhibit parallel ability to activate T-cell subsets. J Allergy Clin Immunol 2011; 128:574-82.
41. Wollenberg A, Kraft S, Hanau D, Bieber T. Immunomorphological and ultrastructural characterization of Langerhans cells and a novel, inflammatory dendritic epidermal cell (IDEC) population in lesional skin of atopic eczema. J Invest Dermatol 1996;106:446-53.
42. Guttman-Yassky E, Lowes MA, Fuentes-Duculan J, Whynot J, Novitskaya I, Cardinale I, et al. Major differences in inflammatory dendritic cells and their products distinguish atopic dermatitis from psoriasis. J Allergy Clin Immunol 2007;119: 1210-7.
43. Watanabe R, Gehad A, Yang C, Scott LL, Teague JE, Schlapbach C, et al. Human skin is protected by four functionally and phenotypically discrete populations of resident and recirculating memory T cells. Sci Transl Med 2015;7:279ra39.
44. Cheuk S, Wiken M, Blomqvist L, Nylen S, Talme T, Stahle M, et al. Epidermal Th22 and Tc17 cells form a localized disease memory in clinically healed psoriasis. J Immunol 2014;192:3111-20.
45. Guttman-Yassky E, Pavel AB, Zhou L, Estrada YD, Zhang N, Xu H, et al. GBR 830, an anti-OX40, improves skin gene signatures and clinical scores in patients with atopic dermatitis. J Allergy Clin Immunol 2019;144:482-93.
46. Shimizu J, Yamazaki S, Takahashi T, Ishida Y, Sakaguchi S. Stimulation of CD25(+)CD4(+) regulatory T cells through GITR breaks immunological self-tolerance. Nat Immunol 2002;3:135-42.
47. Tsoi LC, Rodriguez E, Degenhardt F, Baurecht H, Wehkamp U, Volks N, et al. Atopic dermatitis is an IL-13-dominant disease with greater molecular heterogeneity compared to psoriasis. J Invest Dermatol 2019;139:1480-9.
48. Gittler JK, Shemer A, Suárez-Fariñas M, Fuentes-Duculan J, Gulewicz KJ, Wang CQ, et al. Progressive activation of T(H)2/T(H)22 cytokines and selective epidermal proteins characterizes acute and chronic atopic dermatitis. J Allergy Clin Immunol 2012;130:1344-54.
49. Quaranta M, Knapp B, Garzorz N, Mattii M, Pullabhatla V, Pennino D, et al. Intraindividual genome expression analysis reveals a specific molecular signature of psoriasis and eczema. Sci Transl Med 2014;6:244ra90.
50. Soderhall C, Marenholz I, Kerscher T, Ruschendorf F, Esparza-Gordillo J, Worm M, et al. Variants in a novel epidermal collagen gene (COL29A1) are associated with atopic dermatitis. PLoS Biol 2007;5.
51. Sabatelli P, Gara SK, Grumati P, Urciuolo A, Gualandi F, Curci R, et al. Expression of the collagen VI alpha5 and alpha6 chains in normal human skin and in skin of patients with collagen VI-related myopathies. J Invest Dermatol 2011;131:99-107.
52. Esparza-Gordillo J, Weidinger S, Folster-Holst R, Bauerfeind A, Ruschendorf F, Patone G, et al. A common variant on chromosome 11q13 is associated with atopic dermatitis. Nat Genet 2009;41:596-601.
53. Castro-Giner F, Bustamante M, Ramon Gonzalez J, Kogevinas M, Jarvis D, Heinrich J, et al. A pooling-based genome-wide analysis identifies new potential candidate genes for atopy in the European Community Respiratory Health Survey (ECRHS). BMC Med Genet 2009;10:128.
54. Harazin M, Parwez Q, Petrasch-Parwez E, Epplen JT, Arinir U, Hoffjan S, et al. Variation in the COL29A1 gene in German patients with atopic dermatitis, asthma and chronic obstructive pulmonary disease. J Dermatol 2010;37: 740-2.
55. Naumann A, Soderhall C, Folster-Holst R, Baurecht H, Harde V, Muller-Wehling K, et al. A comprehensive analysis of the COL29A1 gene does not support a role in eczema. J Allergy Clin Immunol 2011;127:1187-94.
56. Strafella C, Caputo V, Minozzi G, Milano F, Arcangeli M, Sobhy N, et al. Atopic eczema: genetic analysis of COL6A5, COL8A1, and COL10A1 in Mediterranean populations. Biomed Res Int 2019;2019:3457898.
57. Suzuki O, Kague E, Bagatini K, Tu H, Heljasvaara R, Carvalhaes L, et al. Novel pathogenic mutations and skin biopsy analysis in Knobloch syndrome. Mol Vis 2009;15:801-9.
58. Gu L, Tseng S, Horner RM, Tam C, Loda M, Rollins BJ. Control of TH2 polarization by the chemokine monocyte chemoattractant protein-1. Nature 2000;404: 407-11.
59. Takamura K, Fukuyama S, Nagatake T, Kim DY, Kawamura A, Kawauchi H, et al. Regulatory role of lymphoid chemokine CCL19 and CCL21 in the control of allergic rhinitis. J Immunol 2007;179:5897-906.
60. Maeda D, Kubo T, Kiya K, Kawai K, Matsuzaki S, Kobayashi D, et al. Periostin is induced by IL-4/IL-13 in dermal fibroblasts and promotes RhoA/ROCK pathway-mediated TGF-beta1 secretion in abnormal scar formation. J Plast Surg Hand Surg 2019;1-7.
61. Ogawa K, Ito M, Takeuchi K, Nakada A, Heishi M, Suto H, et al. Tenascin-C is upregulated in the skin lesions of patients with atopic dermatitis. J Dermatol Sci 2005;40:35-41.
62. Wollenberg A, Howell MD, Guttman-Yassky E, Silverberg JI, Kell C, Ranade K, et al. Treatment of atopic dermatitis with tralokinumab, an anti-IL-13 mAb. J Allergy Clin Immunol 2019;143:135-41.
63. Diaz A, Tan K, He H, Xu H, Cueto I, Pavel AB, et al. Keloid lesions show increased IL-4/IL-13 signaling and respond to Th2-targeting dupilumab therapy. J Eur Acad Dermatol Venereol 2019.
64. Greenblatt MB, Aliprantis AO. The immune pathogenesis of scleroderma: context is everything. Curr Rheumatol Rep 2013;15:297.
65. Dahlgren MW, Jones SW, Cautivo KM, Dubinin A, Ortiz-Carpena JF, Farhat S, et al. Adventitial stromal cells define group 2 innate lymphoid cell tissue niches. immunity 2019;50:707-22.
66. Rana BMJ, Jou E, Barlow JL, Rodriguez-Rodriguez N, Walker JA, Knox C, et al. A stromal cell niche sustains ILC2-mediated type-2 conditioning in adipose tissue. J Exp Med 2019;216:1999-2009.
67. Spallanzani RG, Zemmour D, Xiao T, Jayewickreme T, Li C, Bryce PJ, et al. Distinct immunocyte-promoting and adipocyte-generating stromal components coordinate adipose tissue immune and metabolic tenors. Sci Immunol 2019;4.
68. Park CO, Kupper TS. The emerging role of resident memory T cells in protective immunity and inflammatory disease. Nat Med 2015;21:688-97.
69. Hijnen D, Knol EF, Gent YY, Giovannone B, Beijn SJ, Kupper TS, et al. CD8(+) T cells in the lesional skin of atopic dermatitis and psoriasis patients are an important source of IFN-γ, IL-13, IL-17, and IL-22. J Invest Dermatol 2013;133:973-9.
70. Nograles KE, Zaba LC, Shemer A, Fuentes-Duculan J, Cardinale I, Kikuchi T, et al. IL-22-producing "T22" T cells account for upregulated IL-22 in atopic dermatitis despite reduced IL-17-producing TH17 T cells. J Allergy Clin Immunol 2009;123:1244-52.